THE JOURNAL OF BIOLOGICAL CHEMISTRY VOL. 291, NO. 23, pp. 12394–12407, June 3, 2016

Proteomic Characterization of Inhibitory Synapses Using a Novel pHluorin-tagged γ-Aminobutyric Acid Receptor, Type A ($GABA_A$), α2 Subunit Knock-in Mouse*[S]

Received for publication, March 4, 2016, and in revised form, March 24, 2016 Published, JBC Papers in Press, April 4, 2016, DOI 10.1074/jbc.M116.724443

Yasuko Nakamura[‡], Danielle H. Morrow[‡], Amit Modgil[‡], Deborah Huyghe[‡], Tarek Z. Deeb[‡], Michael J. Lumb[§], Paul A. Davies[‡], and Stephen J. Moss[‡§1]

From the [‡]Department of Neuroscience, Tufts University School of Medicine, Boston Massachusetts 02111 and the [§]Department of Neuroscience, Physiology and Pharmacology, University College, London WC1E 6BT, United Kingdom

The accumulation of γ-aminobutyric acid receptors ($GABA_A$Rs) at the appropriate postsynaptic sites is critical for determining the efficacy of fast inhibitory neurotransmission. Although we know that the majority of synaptic $GABA_A$R subtypes are assembled from α1–3, β, and γ2 subunits, our understanding of how neurons facilitate their targeting to and stabilization at inhibitory synapses is rudimentary. To address these issues, we have created knock-in mice in which the pH-sensitive green fluorescent protein (GFP) and the Myc epitope were introduced to the extracellular domain of the mature receptor α2 subunit (pHα2). Using immunoaffinity purification and mass spectroscopy, we identified a stable complex of 174 proteins that were associated with pHα2, including other $GABA_A$R subunits, and previously identified receptor-associated proteins such as gephyrin and collybistin. 149 of these proteins were novel $GABA_A$R binding partners and included G-protein-coupled receptors and ion channel subunits, proteins that regulate trafficking and degradation, regulators of protein phosphorylation, GTPases, and a number of proteins that regulate their activity. Notably, members of the postsynaptic density family of proteins that are critical components of excitatory synapses were not associated with $GABA_A$Rs. Crucially, we demonstrated for a subset of these novel proteins (including cullin1, ephexin, potassium channel tetramerization domain containing protein 12, mitofusin2, metabotropic glutamate receptor 5, p21-activated kinase 7, and Ras-related protein 5A) bind directly to the intracellular domains of $GABA_A$Rs, validating our proteomic analysis. Thus, our experiments illustrate the complexity of the $GABA_A$R proteome and enhance our understanding of the mechanisms neurons use to construct inhibitory synapses.

$GABA_A$Rs[2] are Cl^--permeable ligand-gated ion channels that mediate the majority of fast synaptic inhibition in the central nervous system (CNS) (1, 2). They are also of therapeutic significance as they are the sites of action for barbiturates, benzodiazepines, general anesthetics, and neuroactive steroids (3). Consistent with their critical roles in regulating neuronal excitability, deficits in the activity of $GABA_A$Rs contribute to a plethora of neurological disorders ranging from anxiety to schizophrenia (4).

Structurally, $GABA_A$Rs can be assembled from 19 different subunits (α1–6, β1–3, γ1–3, δ, ϵ, θ, π, and ρ1–3). The majority of $GABA_A$Rs are believed to be heteropentamers composed of two copies of a single α subunit, two copies of a single β subunit, and one copy of either γ or δ subunits (5, 6). $GABA_A$Rs containing α1–3 and γ are enriched at inhibitory synapses and mediate phasic inhibition, whereas those containing α4–6 and δ are found at extrasynaptic locales and mediate tonic inhibition (1, 2). Notably, subunit composition impacts the pharmacological and physiological properties of these varying receptor subtypes (1, 7, 8). Moreover, $GABA_A$Rs containing unique subunit combinations are selectively targeted to distinct types of inhibitory synapses. However, our understanding of the cellular mechanisms that neurons utilize to regulate $GABA_A$R accumulation at inhibitory synapses is rudimentary. Importantly, the processes that regulate inhibitory synaptogenesis are distinct to those used to build excitatory synapses, which are largely dependent upon PDZ domain-mediated protein-protein interactions (9).

To identify proteins that are relevant for inhibitory synaptogenesis and maintenance, we created knock-in mice in which the pH-sensitive green fluorescent protein (GFP) and the Myc epitope were introduced between amino acids 4 and 5 of the mature $GABA_A$R α2 subunit (pHα2). Following purification on Myc and/or GFP matrices, $GABA_A$R complexes were analyzed by mass spectrometry, and a stable complex of 174 interacting proteins was identified. Importantly, these included the $GABA_A$R α1–5, β1–3, γ1–3, and δ subunits in addition to the previously identified $GABA_A$R-associated proteins gephyrin (Gphn) and collybistin (Arhgef9). However, 149 of these proteins were novel $GABA_A$R binding partners G-protein-coupled receptors (GPCRs); ion channel subunits; regulators of membrane trafficking and protein stability; modulators of protein phosphorylation; GTPases; and related exchange factors. Sig-

* This work was supported by National Institutes of Health Grants NS051195, NS056359, NS081735, R21NS080064, and NS087662 from NINDS (to S. J. M.), National Institute of Mental Health Grant MH097446 (to P. A. D. and S. J. M.), and Department of Defense Grant AR140209 (to P. A. D. and S. J. M.). S. J. M. serves as a consultant for AstraZeneca and SAGE Therapeutics relationships that are regulated by Tufts University and do not impact this study. The content is solely the responsibility of the authors and does not necessarily represent the official views of the National Institutes of Health.

[S] This article contains supplemental Tables S1 and S2.

[1] To whom correspondence should be addressed. Tel.: 617-636-3976; Fax: 617-636-2413; E-mail: Stephen.Moss@Tufts.edu.

[2] The abbreviations used are: $GABA_A$R, γ-aminobutyric acid receptor; Gphn, gephyrin; DGGC, dentate gyrus granule cell; pF, picofarad; sIPSC, spontaneous IPSC; GEF, GDP-GTP exchange factor; IP, immunoprecipitation; coIP, coimmunoprecipitation.

nificantly, these interactions were confirmed using *in vitro* binding coupled with immunoprecipitation. Collectively, these results provide new insights into the components of the $GABA_AR$ proteome.

Experimental Procedures

Animals—All animal protocols were carried out in accordance with the National Institutes of Health Guide for the Care and Use of Laboratory Animals and were approved by Institutional Animal Care and Use Committee of Tufts University.

Antibodies and Expression Constructs—The following antibodies were used for immunocytochemistry: C-terminal anti-α2 antibody was provided by Drs. V. Tretter and W. Sieghart (Medical University of Vienna); anti-gephyrin (1:1000, Synaptic Systems, catalog no. 147021); Alexa Fluor 568 and 647 secondaries (1:1000, Invitrogen). The following antibodies were used for Western blotting: anti-$GABA_AR$ α2 (1:500, PhosphoSolutions, catalog no. 822-GA2C); anti-$GABA_AR$ α4 (1:5000) antisera was raised against the intracellular domain of this subunit (379–421), as described previously (10); anti-$GABA_AR$ β3 (1:1000, PhosphoSolutions, catalog no. 863-GB3C and 1:1000, NeuroMab, catalog no. 75-149); anti-collybistin (1:500, Synaptic Systems, catalog no. 261-003); anti-cul1 (1:2500, Abcam, catalog no. AB75817); anti-ephexin (1:1000, provided by Dr. M. E. Greenberg, Harvard University); anti-GAPDH (1:5000, Santa Cruz Biotechnology, catalog no. SC25778); anti-gephyrin (1:1000, C13B11, Synaptic Systems, catalog no. 147111); anti-GFP (1:1000, Synaptic Systems, catalog no. 132002); anti-Mfn2 (0.5 μg/ml, Abcam, catalog no. 56889); anti-mGluR5 (1:4000, Millipore, AB5675); anti-NR1 (1:1000, BD Biosciences); anti-PAK5 (1:1000, R&D Systems, catalog no. MAB4696); anti-Rab5 (1:1000, Abcam, catalog no. AB18211); anti-tubulin (1:10,000, Millipore, catalog no. 05661); and anti-HRP-conjugated secondary (1:10,000, Jackson ImmunoResearch, catalog nos. 715035150 and 715035152). The following constructs were used: GST fusion protein constructs encoding the large intracellular loop of $GABA_AR$ subunits α1, α2, β3, and γ2 as described previously (11, 12). FLAG-ephexin was provided by M. E. Greenberg (Harvard University), as described previously (13). pHα2 and β3 constructs have been described previously (14, 15), respectively.

Creation of Myc-pHluorin $GABA_AR$ α2 Knock-in Mice—pHα2 mice were generated by homologous recombination in embryonic stem (ES) cells (129Sv/Pas ES cells). A targeting vector was constructed to insert the pHluorin and Myc tag into exon 3 between amino acids 4 and 5 of the mature protein. The targeting vector consisted of a neomycin-positive selection cassette in intron 2 found ~250 bp upstream of exon 3. An HSV-thymidine kinase-negative selection cassette was positioned at the 5′ end of the construct. The targeting vector was electroporated into 129Sv ES cells, and clones were screened by PCR and Southern blot analysis. ES cell clones were then expanded and selected for C57BL/6J blastocyst injections. The resulting chimeras were bred with wild type C57BL/6J mice. The neomycin cassette was subsequently excised by breeding with Cre mice.

Cresyl Violet Stain—pHα2 and WT mice (8–10 weeks old) were transcardially perfused with PBS followed by 2% paraformaldehyde in PBS. Dissected brains were post-fixed overnight and transferred to 30% sucrose solution. Brains were subsequently sliced into 40-μm sections and stored in cryoprotectant (30% sucrose, 30% ethylene glycol, 1% polyvinylpyrrolidone in PBS) at −20 °C until use. Sections were washed with PBS before processing. Slide-mounted sections were sequentially washed in 100% ethanol, 95% ethanol, distilled H_2O and stained with cresyl violet (0.3% glacial acetic acid, 0.5% cresyl violet acetate). This was followed by further rinses in 95% ethanol, 100% ethanol and xylene. Images were acquired with Nikon E800 microscope at 1600 × 1200 resolution using a ×4 objective. Twelve sections and three animals per genotype were imaged.

Western Blot Analysis—Proteins separated by SDS-PAGE (8–10% gel) were transferred to PVDF membranes and blocked in 6% milk in PBST for 1 h. Membranes were further incubated with the appropriate primary antibody (5% milk in PBST), and after extensive washes, they were probed with HRP-conjugated secondary antibodies for 1 h. Western blots were developed using an enhanced chemiluminescence system as per the manufacturer's instructions (Amresco). Membranes were imaged (ChemiDoc MP, Bio-Rad) and analyzed using ImageJ (National Institutes of Health). Two-tailed unpaired *t* test or analyses of variance with Games-Howell post hoc test (for multiple comparisons with unequal variances) were performed to analyze data (GraphPad, SPSS). Graphs presented show means ± S.E. of the mean (S.E.).

Immunocytochemistry—Hippocampal neurons were prepared from E18 to E19 pHα2 mice and were used for experiments at 18 days *in vitro*. For immunocytochemistry experiments, cultures were fixed in 4% paraformaldehyde, 5% sucrose, permeabilized, and probed for the $GABA_AR$ α2 subunit and gephyrin and were subsequently stained with Alexa Fluor secondary antibodies. 3–5 neurons were imaged from three independent cultures.

Fixed-cell images were acquired using a Nikon Eclipse Ti confocal microscope. Images were taken at 1024 × 1024 resolution with a ×60 objective. Calculation of the Pearson's coefficient was performed with the JaCOP (16) plugin for ImageJ software (17).

Coimmunoprecipitation (coIP)—To detect bound gephyrin and collybistin, brains were removed from isoflurane-anesthetized mice (8–10 weeks). Hippocampi from WT and pHα2 mice were lysed in lysis buffer containing 20 mM Tris-HCl, pH 8.0, 150 mM NaCl, 2% Triton X-100, 5 mM EDTA, 10 mM NaF, 2 mM Na_3VO_4, 10 mM $Na_4P_2O_7$, plus protease inhibitors. These samples were spun at 16,100 × *g* for 15 min at 4 °C, and the supernatant (or lysate) was incubated with 3 μg of Myc antibody overnight in lysis buffer (modified to 1% Triton X-100). The addition of protein G-Sepharose beads (GE Healthcare) for 4 h was followed by four quick washes (400 × *g*, 2 min, 4 °C) in 1.5 ml of lysis buffer. For GFP IPs, GFP-Trap beads (Chromotek, catalog no. Gta-200) were incubated with hippocampal lysate overnight. Bound proteins were detected by Western blotting. To detect bound mGluR5, KCTD12, and ephexin, hippocampal/cortical lysates prepared as above were pre-cleared overnight with agarose beads conjugated to IgG. These samples were incubated with GFP-Trap for 2 h and subsequently washed three times for 10 min in 1.5 ml of lysis buffer (modified to 0.2% Triton X-100 and centrifuged at 2500 × *g*, 2 min, 4 °C).

Bound proteins were detected by Western blotting. For experiments using HEK293 cells, pre-cleared lysates were incubated with anti-FLAG conjugated beads (Sigma, catalog no. F3165) or GFP-Trap for 2 h and subsequently washed four times in lysis buffer. Bound proteins were detected by Western blotting. A minimum of three independent experiments were performed for all coIP experiments.

Hippocampal Slice Preparation for Electrophysiology Recordings—Coronal slices were prepared from male WT and pHα2 animals (8–10 weeks old). Isoflurane-anesthetized mice were decapitated, and brains were rapidly removed and put in an ice-cold cutting solution (126 mM NaCl, 2.5 mM KCl, 0.5 mM $CaCl_2$, 2 mM $MgCl_2$, 26 mM $NaHCO_3$, 1.25 mM NaH_2PO_4, 10 mM glucose, 1.5 mM sodium pyruvate, and 3 mM kynurenic acid). 310-μm slices cut with a vibratome VT1000S (Leica Microsystems, St Louis, MO) were transferred to an incubation chamber filled with warmed (31 °C) oxygenated artificial cerebrospinal fluid (ACSF: 126 mM NaCl, 2.5 mM KCl, 2 mM $CaCl_2$, 2 mM $MgCl_2$, 26 mM $NaHCO_3$, 1.25 mM NaH_2PO_4, 10 mM glucose, 1.5 mM sodium pyruvate, 1 mM glutamine, 3 mM kynurenic acid, and 5 μM GABA) and bubbled with 95% O_2 to 5% CO_2. Slices were allowed to recover for 1 h before recording.

Electrophysiology Recordings—After recovery, slices were transferred to a submerged recording chamber on the stage of an upright microscope (Nikon FN-1) with a ×40 water immersion objective equipped with DIC/IR optics. Slices were gravity-superfused with ACSF solution throughout experimentation and perfused at a rate of 2 ml/min with oxygenated (O_2/CO_2 95:5%) ACSF at 32 °C. Adequate O_2 tension and pH 7.3–7.4 values were maintained by continuously bubbling the media with 95% O_2, 5% CO_2. Currents were recorded from the dentate gyrus granule cells (DGGCs) in coronal hippocampal slices. Patch pipettes (5–7 megohms) were pulled from borosilicate glass (World Precision Instruments) and filled with intracellular solution (140 mM CsCl, 1 mM $MgCl_2$, 0.1 mM EGTA, 10 mM HEPES, 2 mM Mg-ATP, 4 mM NaCl, and 0.3 mM Na-GTP, pH 7.25). A 5-min period for stabilization after obtaining the whole-cell recording configuration was allowed before currents were recorded using an Axopatch 200B amplifier (Molecular Devices), low pass-filtered at 2 kHz, digitized at 20 kHz (Digidata 1440A; Molecular Devices), and stored for off-line analysis. The holding potential was −60 mV for all recordings.

Electrophysiology Analysis—Tonic current measurements were measured from an all-points histogram that was plotted for a 10-s period before and during picrotoxin application. A Gaussian fit to these points gave the mean current amplitude, and the difference between these two values was considered to be the tonic current and normalized to cell capacitance (pA/pF). Throughout the course of the experiment, series resistance and whole-cell capacitance were continually monitored and compensated. If series resistance increased by >20%, recordings were eliminated from the data analysis. Statistical significance was determined using Student's *t* test. Spontaneous IPSCs (sIPSCs) were analyzed using the mini-analysis software (version 5.6.4; Synaptosoft, Decatur, GA). sIPSCs were recorded for a minimum of 5 min. To detect sIPSCs, the minimum threshold detection was set to three times the value of baseline noise signal. The recording trace was visually inspected, and only sIPSC events with a stable baseline, sharp rising phase, and single peak were used to negate artifacts due to event summation. Only recordings with a minimum of 100 events fitting these criteria were analyzed. 8–10 cells were recorded from three animals of each genotype. Amplitude, decay, and frequency distributions of sIPSCs were examined by constructing all-point cumulative probability distributions and compared using the Mann-Whitney test and Kolmogorov-Smirnov test. Values of $p < 0.05$ were considered significant.

Large Scale Immunoprecipitation for Mass Spectrometry Analysis—Hippocampus and cortex of age-matched (8–10 weeks) and sex-matched WT and pHα2 mice (seven animals each) were prepared as above. Lysates were filtered and pre-cleared with agarose beads conjugated to IgG overnight. For tandem IPs, pre-cleared lysates were incubated with Myc antibody overnight. Sepharose beads were added and incubated at 4 °C for 4 h. These beads were washed (three times at 400 × *g*, 2 min, 4 °C), and the proteins were eluted off beads with 200 μg/ml c-Myc peptide (Alpha Diagnostics) in lysis buffer. The eluate was incubated with GFP-Trap for 1 h, followed by four washes (2500 × *g*, 2 min, 4 °C) in lysis buffer. Gels were run and stained with silver stain (Sigma), and gel bands of interest from pHα2 and the corresponding regions from WT mice were excised. For single IPs, pre-cleared lysates were incubated with GFP-Trap for 2 h, followed by four washes in lysis buffer (2500 × *g*, 2 min, 4 °C). Gels were run and stained with colloidal Coomassie (18). Each gel lane (for pHα2 or WT IP) was cut into five pieces and sent to Taplin Mass Spectrometry Facility (Harvard University) for proteomic analysis.

Mass Spectrometry Analysis—Trypsin digestion, liquid chromatography-tandem mass spectrometry (LC-MS/MS), and MS/MS spectra search in a mouse database (Uniprot) using the Sequest 28 analysis program was performed by Taplin Mass Spectrometry Facility (Harvard University). Peptide matches were considered true matches for ΔCN scores (Δ correlation) >0.2 and XCorr values (cross-correlation) of greater than 2, 2, 3, 4 for +1, +2, +3, +4 charged peptides, respectively (supplemental Tables 1 and 2). A particular protein would only be considered present if at least five such high quality peptides were detected. Three independent mass spectrometry experiments were performed. Proteins identified in pHα2 mice were compared with those found in WT animals to control for nonspecific binding of proteins. Proteins found at similar levels to a list of nonspecific binding proteins often found in mass spectrometry experiments were removed (19). For tandem IP experiments, proteins were identified by a minimum of seven peptides. Peptides found in WT control IPs were removed from the final list of proteins displayed in Table 1. For GFP-Trap IPs, proteins listed in Tables 2–7 have been identified by a minimum of five peptide, or were at least 3-fold enriched in the pHα2 compared with WT IPs. Furthermore, these peptides were present in all three experiments. Proteins in Tables 2–7 were manually organized into broad functions through information from GeneCards, HUGO gene nomenclature committee, and the literature.

Glutathione S-transferase (GST) Production and Pulldown Assay—GST fusion proteins expressed in *Escherichia coli* BL21 were induced (0.2 mM isopropyl 1-thio-β-D-galactopyranoside, 2 h), pelleted, and resuspended in buffer A (10 mM Tris-Cl, pH

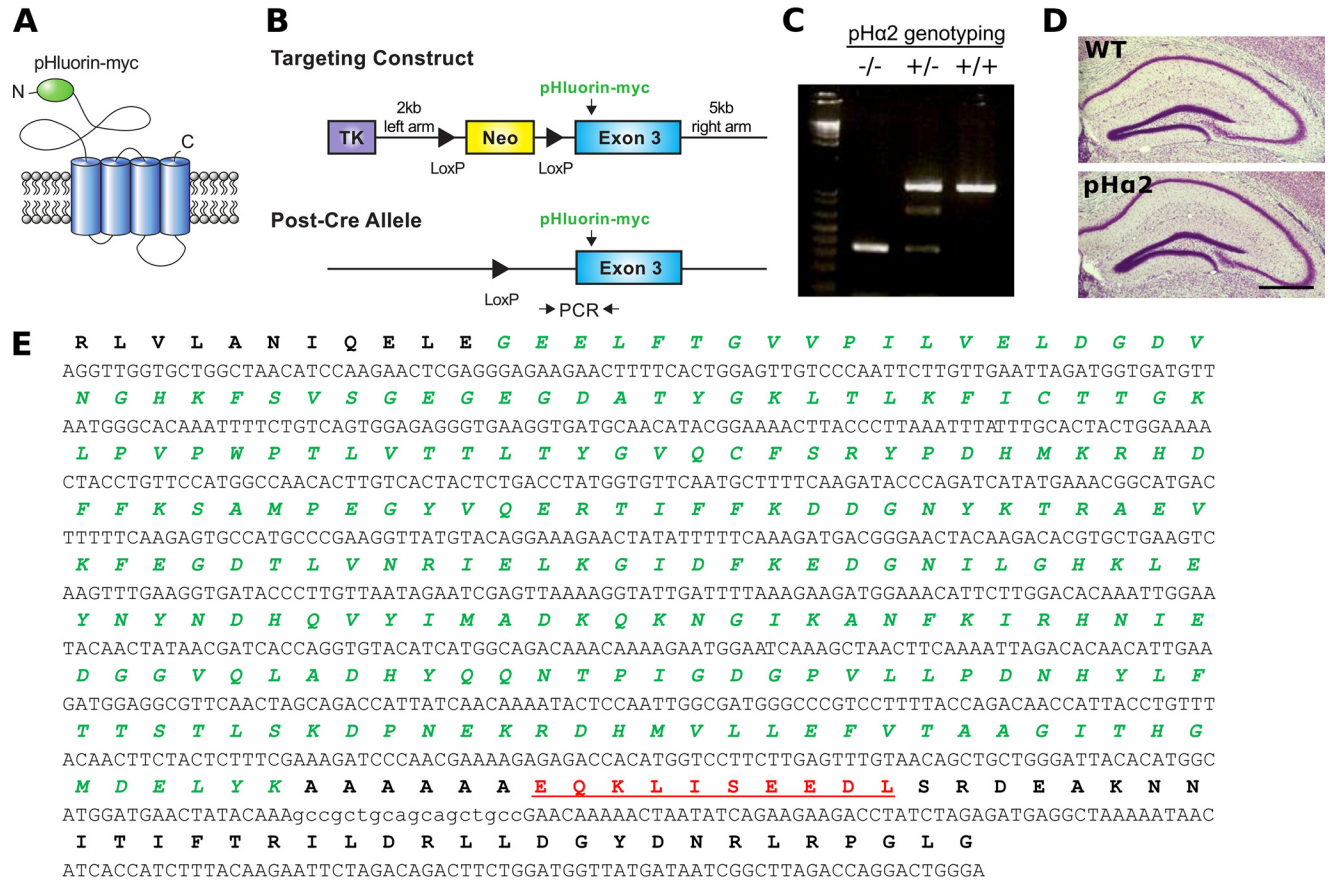

FIGURE 1. **Construction of pHluorin-Myc-tagged GABA$_A$R α2 mouse.** *A*, schematic representation of pHluorin-Myc tagged at the N terminus of the GABA$_A$R α2 subunit. *B*, illustrations of the targeting vector and the targeted α2 subunit gene with addition of pHluorin-myc into exon 3. *C*, genotyping for wild type (−/−), heterozygotes (+/−), and pHα2 (+/+) mice using primers flanking pHluorin. *D*, cresyl violet staining of hippocampus shows there are no gross morphological changes in the hippocampal anatomy of pHα2 mice. *Scale bar*, 500 μm. *E*, DNA and protein sequence of N-terminal segment of pHα2 knock-in mouse. pHluorin (*green, italics*) and Myc (*red, underline*) reporters are depicted.

7.4, 1 mM EDTA, pH 8.0, 1% Triton X-100). After sonication, 2.5× buffer B was added (20 mM HEPES, 100 mM KCl, 0.2 mM EDTA, 20% glycerol), and the lysate was spun down. Supernatants containing GST fusion proteins were immobilized on preswollen glutathione-agarose beads (Sigma). Beads were washed five times with buffer B and kept frozen until use.

Hippocampal and cortical lysates (prepared as above) from male WT mice were pre-cleared with GST alone. These samples were then incubated with GST tagged to various GABA$_A$R subunits immobilized on glutathione-agarose beads overnight. Beads were washed three times (400 × *g*, 2 min, 4 °C), and bound proteins were detected by immunoblotting. A minimum of three independent GST experiments was performed for each protein studied.

Human Embryonic Kidney 293 (HEK293) Cell Transfection—HEK293 cells were maintained in DMEM (Gibco) supplemented with 10% FBS (Gibco) and 1% penicillin/streptomycin (Gibco) at 37 °C and 5% CO_2. HEK293 cells were cotransfected by electroporation (Bio-Rad) with 3 μg of plasmid DNA per construct 40–48 h before experimentation.

Results

Creation of a pHluorin/Myc-tagged GABA$_A$R α2 Subunit Knock-in Mouse—To date, our understanding of the mechanisms responsible for the formation and maintenance of inhibitory synapses has been limited. These issues are confounded by the structural diversity of GABA$_A$Rs and technical limitations such as the paucity of high affinity subunit-selective antibodies. To overcome these limitations, mice were created in which pHluorin, a pH-sensitive GFP, and the Myc epitope (EQKLISEEDL, Fig. 1, *A* and *E*) were introduced into the GABA$_A$R α2 subunit. These reporters were introduced into exon 3 of the GABA$_A$R α2 subunit gene between the codons encoding amino acids 4 and 5 of the mature protein (pHα2). This location was chosen because studies in expression systems suggest that the respective modifications are functionally silent (14, 20). pHα2 mice were created using homologous recombination in ES cells, blastocyst injection, and Cre-mediated excision of the neomycin selection marker (Fig. 1*B*). Mice were genotyped by PCR using primers that detect the presence of pHluorin insertion (Fig. 1*C*), and the respective mice were backcrossed on the C57BL/6J background in excess of 10 generations. The presence of the pHluorin and Myc reporters was confirmed by DNA sequencing (Fig. 1*E*).

pHα2 Subunit Is Associated with Endogenous GABA$_A$R Subunits and Known Receptor-associated Proteins—pHα2 homozygotes were viable, bred normally, and did not exhibit any overt phenotypes. In addition, Nissl staining did not reveal any gross abnormalities in the structure of the hippocampus between WT and pHα2 mice (Fig. 1*D*). To confirm the expres-

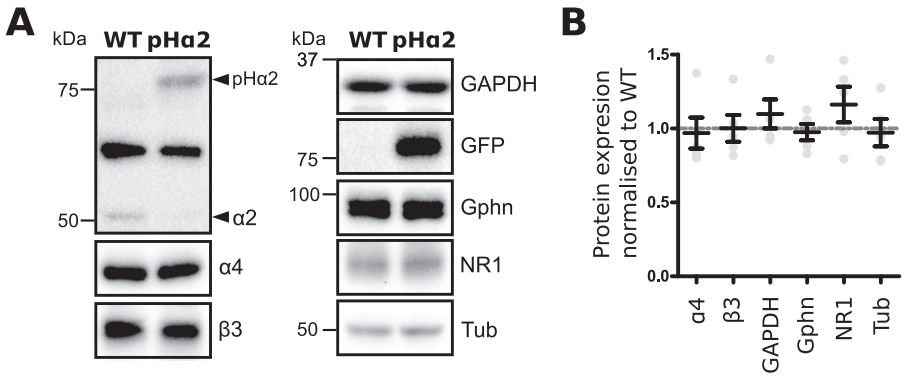

FIGURE 2. **Characterization of pHα2 mice.** *A,* representative Western blots of hippocampal lysates from WT and pHα2 mice. The pHluorin-Myc tag increases the molecular weight of the GABA$_A$R α2 subunit. *B,* pooled quantification of protein expression shows there are no significant differences in the total expression levels of GABA$_A$R α4 ($p = 0.80$, *t* test, $n = 5$), β3 ($p = 0.78$, *t* test, $n = 5$), GAPDH ($p = 0.99$, *t* test, $n = 4$), gephyrin ($p = 0.46$, *t* test, $n = 5$), NMDAR NR1 ($p = 0.09$, *t* test, $n = 5$), and tubulin (*Tub*) ($p = 0.99$, *t* test, $n = 4$) between the two genotypes. Data represent means ± S.E.

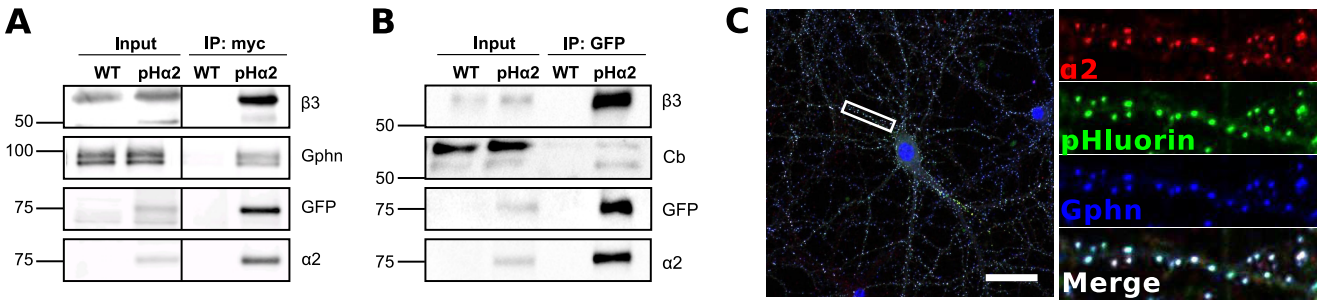

FIGURE 3. **Localization of pHα2 at inhibitory synaptic sites.** Gephyrin, collybistin, and the GABA$_A$R β3 subunit coIP with pHα2. Hippocampal lysates from WT and pHα2 mice were incubated with Myc (*A*) or GFP (*B*) antibody, and bound proteins were detected by Western blotting. Immunoprecipitated pHα2 (GFP and α2 bands at ~75 kDa) coimmunoprecipitated with GABA$_A$R β3, gephyrin (*Gphn*), and collybistin (*Cb*). *C,* hippocampal neurons from pHα2 mice were stained for GABA$_A$R α2 (*red*) and the inhibitory synaptic marker gephyrin (*blue*). Endogenous pHluorin fluorescence (*green*) colocalized with GABA$_A$R α2 (Pearson's coefficient α2 0.89 ± 0.02, $p < 0.001$) and gephyrin (Pearson's coefficient gephyrin 0.76 ± 0.02, $p < 0.005$) staining at inhibitory synapses. $n = 12$ cells taken from three separate cultures. *Scale bar,* 30 μm.

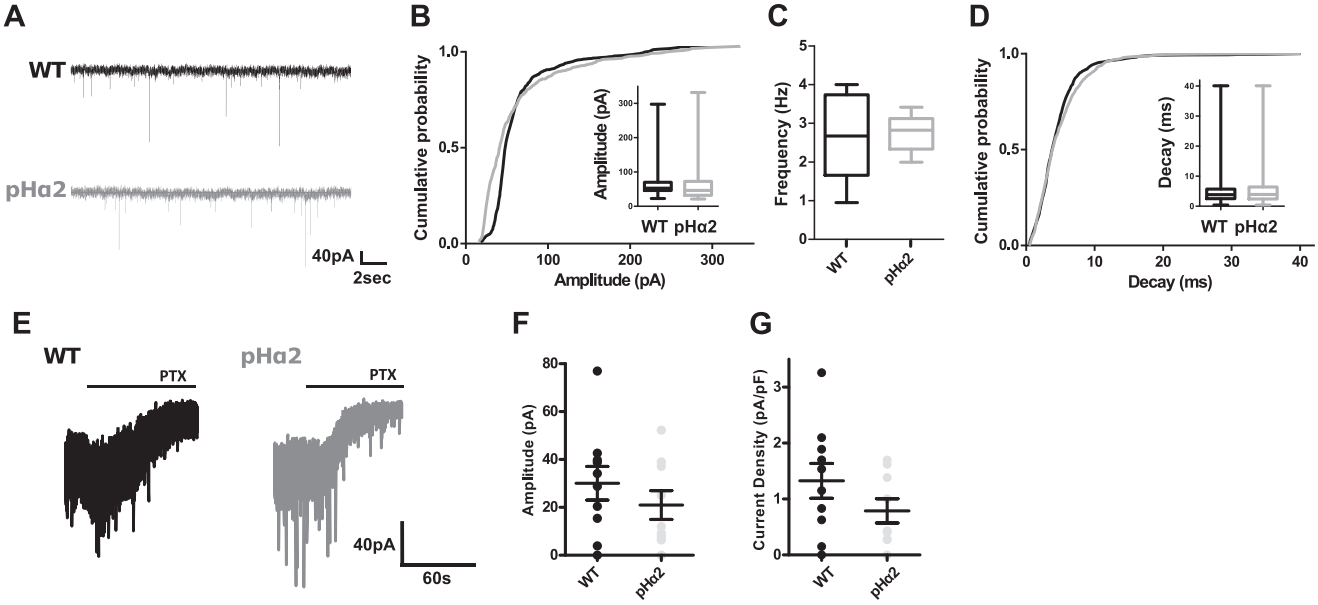

FIGURE 4. **Phasic and tonic inhibition are unperturbed in pHα2 mice.** sIPSCs recorded from DGGCs of WT (*black*) and pHα2 (*gray*) mice (*A*) show no significant differences in their amplitude ($p = 0.06$, Kolmogorov-Smirnov test, $n = 8$ cells) (*B*), frequency ($p > 0.99$, Mann Whitney test, $n = 8$) (*C*), and decay time ($p = 0.82$, Kolmogorov-Smirnov test, $n = 8$) (*D*). Tonic current in DGGCs display no differences in amplitude ($p = 0.34$, *t* test, $n = 9–10$) (*E*) and current density ($p = 0.18$, *t* test, $n = 9–10$) (*F*) between genotypes (*G*).

sion of the pHα2 subunit, immunoblotting was utilized with α2 subunit antibodies. In accordance with the addition of pHluorin, the molecular mass of the α2 subunit was increased by ~30 kDa in extracts prepared from pHα2 homozygotes compared with WT (Fig. 2*A*). However, there were no significant differences in the total expression levels of the GABA$_A$Rs α4 and β3

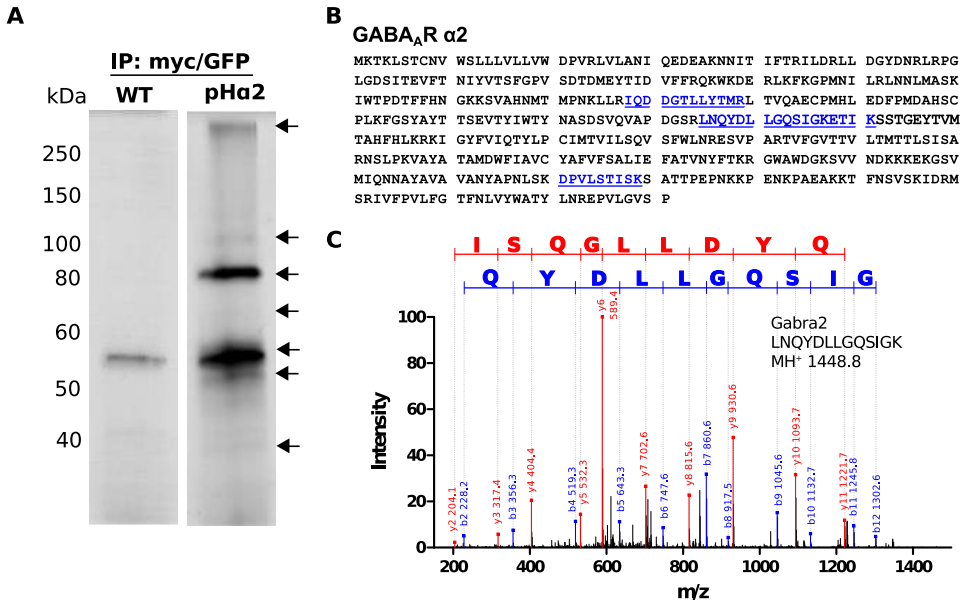

FIGURE 5. **Two-step purification to isolate pHα2 complexes.** Detergent-solubilized hippocampal and cortical lysates of age- and sex-matched WT and pHα2 mice were immunoprecipitated with Myc followed by GFP-Trap and subjected to SDS-PAGE and silver staining (*A*). Representative silver-stained gel depicts bands of interest (*arrow*) that were excised from pHα2 and the corresponding WT lane for mass spectrometry analysis. Protein coverage of GABA$_A$R α2 subunit (*blue, underline*) identified by MS analysis (*B*). Example of MS/MS spectrum for tryptic peptide identified as GABA$_A$R α2 is shown (*C*). The sequence of the identified peptide is indicated.

subunit, GAPDH, gephyrin, NMDA receptor NR1 subunit, and tubulin in pHα2 mice compared with wild type animals (Fig. 2*B*; $p > 0.05$).

Plasma membrane accumulation of the α2 subunit is dependent upon oligomerization with receptor β subunits (1, 2, 21). To test whether pHα2 subunits are associated with endogenous receptor β subunits, detergent-solubilized brain extracts were subjected to immunoprecipitation with Myc or GFP antibodies. As measured by immunoblotting, the α2 and β3 subunits were detected to immunoprecipitate with Myc or GFP antibodies from pHα2 but not WT brains (Fig. 3, *A* and *B*). Molecular, genetic, and biochemical approaches suggest that the multifunctional protein gephyrin and the GDP-GTP exchange factor collybistin play important roles in determining the synaptic accumulation of GABA$_A$Rs (1, 2, 12, 22). Consistent with this, both of these proteins were detected to immunoprecipitate with Myc/GFP antibodies from pHα2 but not WT brain extracts. Thus, in mouse brain pHα2 assembles with endogenous GABA$_A$R subunits and is associated with gephyrin and collybistin.

pHα2 Subunits Are Targeted to Functional Inhibitory Synapses—In the brain, GABA$_A$Rs containing α2 subunits are highly concentrated at inhibitory synapses (1, 2, 23, 24). To assess whether this synaptic targeting also occurs in pHα2 mice, 18 days *in vitro* hippocampal cultures produced from these mice were stained with α2 and gephyrin antibodies and imaged by confocal microscopy. Endogenous green fluorescence colocalized with GABA$_A$R α2 subunit immunoreactivity (Fig. 3*C*; $p < 0.001$) at gephyrin-positive postsynaptic inhibitory specializations (Fig. 3*C*; $p < 0.005$).

Next, we compared the properties of phasic and tonic inhibition in the dentate gyrus granule cells (DGGCs) of WT and pHα2 mice (Fig. 4). Examination of sIPSCs revealed that there was no significant difference in the amplitude (Fig. 4*B*; WT 68.7 ± 1.6 pA, $n = 8$; pHα2 67.3 ± 2.0 pA, $n = 8$, $p = 0.06$), frequency (Fig. 4*C*; WT 2.7 ± 0.4 Hz, $n = 8$; pHα2 2.8 ± 0.2 Hz, $n = 8$, $p > 0.99$), and decay time (Fig. 4*D*; WT 4.6 ± 0.1 ms, $n = 8$; pHα2 4.9 ± 0.1 ms, $n = 8$, $p = 0.82$) between genotypes. Similarly, the tonic current amplitude (Fig. 4*F*; WT 30.1 ± 7.0 pA, $n = 9$; pHα2 21.0 ± 6.0 pA, $n = 10$, $p = 0.34$) and current density (Fig. 4*G*; WT 1.3 ± 0.3 pA/pF $n = 10$; pHα2 0.8 ± 0.2 pA/pF $n = 9$, $p = 0.18$) were comparable between WT and pHα2 mice.

Collectively, these data suggest that GABA$_A$Rs containing pHα2 subunits are targeted to inhibitory synapses, and their incorporation at these subcellular specializations does not have an impact on GABAergic inhibition.

Isolation of GABA$_A$Rs from the Brains of pHα2 Mice Using Two-step Tandem Affinity Purification—To assess which proteins associate with GABA$_A$R subunits in the brain, a two-step immunoaffinity purification protocol was performed. First, hippocampi and cortices from age/sex-matched WT and pHα2 mice were solubilized and exposed to Myc antibody followed by binding to G-Sepharose beads. After extensive washes, bound material was eluted with Myc peptide and exposed to immobilized GFP-Trap beads. Bound material was subsequently eluted using 2% SDS and subjected to SDS-PAGE followed by silver staining. Bands that were present in the pHα2 lane and the adjacent lane from WT mice were excised and subjected to LC-MS/MS (Fig. 5). Three independent purifications were performed for both WT controls and pHα2 animals. Table 1 shows a list of the proteins identified by MS analysis that associate with pHα2. Proteins listed were identified by a minimum of seven peptides. Furthermore, proteins that bound non-specifically (in WT controls) were removed. Using these criteria, the GABA$_A$R α1, α3, α4, α5, β1, β2, β3, and γ2 subunits in addition to the α1 subunit of the Na^+/K^+-ATPase subunit copurified with the pHα2 (Table 1 and supplemental Table 1). Although

TABLE 1

Proteins identified with pHα2 identified using tandem myc/GFP-Trap purification

Summary of MS/MS analysis results of proteins associated with pHα2 after purification using Myc and pHluorin tag from three independent experiments. Age- and sex-matched WT mice were used as controls for non-specific binding of proteins. Total peptides indicate the sum of peptides found in all experiments.

Gene symbol	Reference	Name	Total peptide	
			WT	pHα2
	GFP-Aequorea	Green fluorescent protein	0	34
Atp1a1	ATA1_MOUSE	Na^+/K^+-transporting ATPase subunit α1	0	9
Gabra1	GBRA1_MOUSE	GABA$_A$R, subunit α1	0	70
Gabra2	GBRA2_MOUSE	GABA$_A$R, subunit α2	0	15
Gabra3	GBRA3_MOUSE	GABA$_A$R, subunit α3	0	8
Gabra4	GBRA4_MOUSE	GABA$_A$R, subunit α4	0	14
Gabra5	GBRA5_MOUSE	GABA$_A$R, subunit α5	0	11
Gabrb1	GBRB1_MOUSE	GABA$_A$R, subunit β1	0	23
Gabrb2	GBRB2_MOUSE	GABA$_A$R, subunit β2	0	17
Gabrb3	GBRB3_MOUSE	GABA$_A$R, subunit β3	0	40
Gabrg2	GBRG2_MOUSE	GABA$_A$R, subunit γ2	0	10

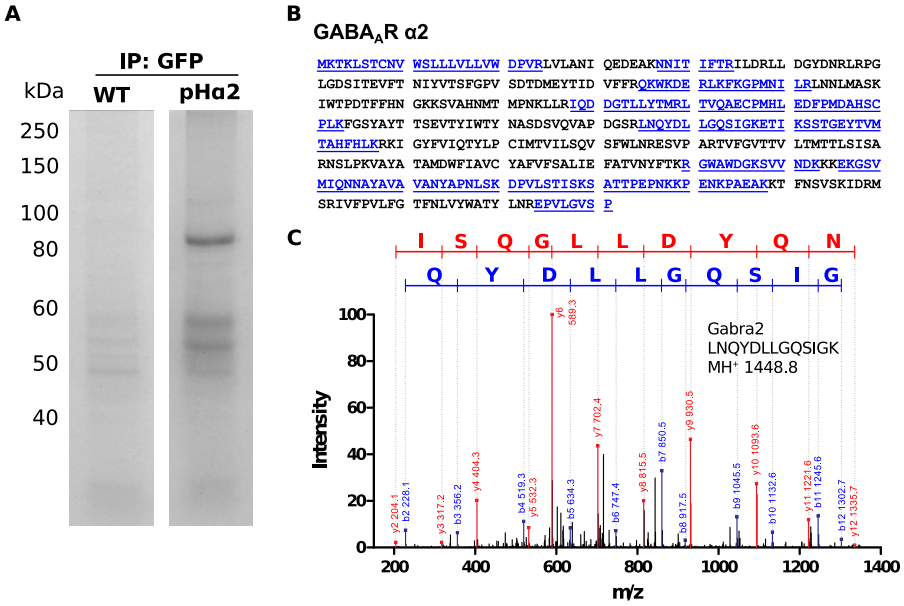

FIGURE 6. **Single-step purification to isolate pHα2 complexes.** Detergent-solubilized hippocampal and cortical lysates from WT and pHα2 mice were immunoprecipitated with GFP antibodies and subjected to SDS-PAGE and colloidal Coomassie staining (*A*). Each gel lane was cut into five pieces and pooled for mass spectrometry analysis. Protein coverage of GABA$_A$R α2 subunit (*blue, underline*) identified by MS analysis (*B*). Example of MS/MS spectrum for tryptic peptide identified as GABA$_A$R α2 is shown (*C*). The sequence of the identified peptide is indicated.

there was some contamination between bands, the majority of GFP and α2 subunit peptides were identified in the major silver-stained product at ~80 kDa. Atp1a1 was found at the 100-kDa region, α4 subunit at the 65-kDa region, and the rest were found in the 50–55-kDa region of the gel. Collectively, these results suggest that pHα2 is capable of assembling with the γ2 and multiple α and β subunit isoforms in the brain.

GFP-Trap Purification of GABA$_A$Rs Reveals Their Association with Known Binding Partners—To increase the probability of identifying proteins that are associated with the α2-containing GABA$_A$Rs, a single purification with GFP-Trap was used. Lysates from hippocampi and cortices of age- and sex-matched WT and pHα2 mice were incubated with GFP-Trap beads. These samples were then subjected to SDS-PAGE followed by Coomassie staining (Fig. 6). The single step purification method led to an increased yield of protein compared with the tandem purification as indicated by the increased number of peptides identified and greater protein coverage for GABA$_A$R α2 (Figs. 5*B* and 6*B*; GFP/myc IP 8.4%, GFP IP 43%). Three independent purifications were performed, and proteins identified by LC-MS/MS in all three experiments and found to be at least 3-fold enriched in the pHα2 samples are listed in Tables 2–7 and supplemental Table 2.

In common with tandem affinity purification, the single-step GFP purification resulted in the isolation of the GABA$_A$R α1–5, β1–3, and γ2 subunits. However, in addition, the single step purification resulted in the isolation of γ1, γ3, and δ subunits (Table 2). Furthermore, a number of other previously verified interactions were confirmed, including binding of GABA$_A$Rs or their closely associated proteins to gephyrin (*Gphn*), collybistin (*Arhgef9*), neuroligins 1–4 (*Nlgn*), PKC isoforms (*Prkc*), PKA (*Prkacb*), GABA$_B$R2 (*Gabbr2*), and glycine receptor β (*Glrb*) as described previously (12, 22, 25–31). Crucially, a key component of excitatory synapses, the highly abundant PSD95 family of proteins (32), was absent from these purifications.

Identification of Novel Components of the GABA$_A$R Proteome Using GFP-Trap Purification—In addition to known interacting proteins as detailed in Table 2, 149 novel binding partners for GABA$_A$Rs were identified in material purified from pHα2 animals. For brevity, these proteins were divided into five

TABLE 2

Known binding partners of GABA$_A$R subunits and their closely associated proteins identified using GFP-Trap purification

Proteins associated with pHα2 were purified using pHluorin tag from three independent experiments. Age- and sex-matched WT mice were used as controls for non-specific binding of proteins. Proteins listed have appeared in all three experiments, have been identified by a minimum of five peptides, and there is a 3-fold difference between peptides found in pHα2 compared with WT IPs.

Gene symbol	Reference	Name	Total peptide	
			WT	pHα2
	GFP_Aequorea	Green fluorescent protein	2	855
Arhgef9	ARHG9_MOUSE	Cdc42 guanine nucleotide exchange factor 9, collybistin	1	62
Gabbr2	GABR2_MOUSE	γ-Aminobutyric acid (GABA) B receptor, 2	2	16
Gabra1	GBRA1_MOUSE	γ-Aminobutyric acid (GABA) A receptor, α1	10	501
Gabra2	GBRA2_MOUSE	γ-Aminobutyric acid (GABA) A receptor, α2	5	341
Gabra3	GBRA3_MOUSE	γ-Aminobutyric acid (GABA) A receptor, α3	3	266
Gabra4	GBRA4_MOUSE	γ-Aminobutyric acid (GABA) A receptor, α4	1	369
Gabra5	GBRA5_MOUSE	γ-Aminobutyric acid (GABA) A receptor, α5	3	146
Gabrb1	GBRB1_MOUSE	γ-Aminobutyric acid (GABA) A receptor, β1	7	481
Gabrb2	GBRB2_MOUSE	γ-Aminobutyric acid (GABA) A receptor, β2	6	293
Gabrb3	GBRB3_MOUSE	γ-Aminobutyric acid (GABA) A receptor, β3	7	422
Gabrd	GBRD_MOUSE	γ-Aminobutyric acid (GABA) A receptor, δ	0	80
Gabrg1	GBRG1_MOUSE	γ-Aminobutyric acid (GABA) A receptor, γ1	0	112
Gabrg2	Q3UVW2_MOUSE	γ-Aminobutyric acid (GABA) A receptor, γ2	0	9
Gabrg2	GBRG2_MOUSE	γ-Aminobutyric acid (GABA) A receptor, γ2	1	198
Gabrg3	GBRG3_MOUSE	γ-Aminobutyric acid (GABA) A receptor, γ3	0	56
Glrb	GLRB_MOUSE	Glycine receptor β	0	6
Gphn	GEPH_MOUSE	Gephyrin	5	140
Nlgn1	NLGN1_MOUSE	Neuroligin 1	2	59
Nlgn2	NLGN2_MOUSE	Neuroligin 2	0	117
Nlgn3	NLGN3_MOUSE	Neuroligin 3	4	33
Nlgn4l	NLGN4_MOUSE	Neuroligin 4	0	6
Prkacb	KAPCB_MOUSE	Protein kinase, cAMP-dependent, β catalytic subunit	1	7
Prkca	KPCA_MOUSE	Protein kinase C, α	15	55
Prkcg	KPCG_MOUSE	Protein kinase C, γ	27	95

TABLE 3

G-protein-coupled receptors, ion channels, and transporters associated with pHα2 identified using GFP-Trap purification

Gene symbol	Reference	Name	Total peptide	
			WT	pHα2
Abcf2	ABCF2_MOUSE	ATP binding cassette subfamily F member 2	1	7
Abcf3	ABCF3_MOUSE	ATP binding cassette subfamily F member 3	2	14
Bai1	BAI1_MOUSE	Adhesion of G protein-coupled receptor B1	0	6
Bai2	BAI2_MOUSE	Adhesion of G protein-coupled receptor B2	0	7
Cacna1e	CAC1E_MOUSE	Calcium channel, voltage-dependent, R type, α1E subunit	1	15
Cacnb1	CACB1_MOUSE	Calcium channel, voltage-dependent, β1 subunit	0	17
Cacnb3	CACB3_MOUSE	Calcium channel, voltage-dependent, β3 subunit	1	14
Cacnb4	CACB4_MOUSE	Calcium channel, voltage-dependent, β4 subunit	4	13
Grm5	GRM5_MOUSE	Glutamate receptor, metabotropic 5	0	6
Kcna1	KCNA1_MOUSE	Potassium channel, voltage-gated shaker-related subfamily A, member 1	2	24
Kcna2	KCNA2_MOUSE	Potassium channel, voltage-gated shaker-related subfamily A, member 2	2	9
Kcna3	KCNA3_MOUSE	Potassium channel, voltage-gated shaker-related subfamily A, member 3	0	8
Kcnb1	KCNB1_MOUSE	Potassium channel, voltage-gated Shab-related subfamily B, member 1	1	7
Lphn3	LPHN3_MOUSE	Adhesion G protein-coupled receptor L3	0	10
Slc1a1	EAA3_MOUSE	Solute carrier family 1 (neuronal/epithelial high affinity glutamate transporter, system Xag), member 1	0	7
Slc1a3	EAA1_MOUSE	Solute carrier family 1 (glial high affinity glutamate transporter), member 3	18	55
Slc24a2	Q14BI1_MOUSE	Solute carrier family 24 (sodium/potassium/calcium exchanger), member 2	0	13
Slc25a11	M2OM_MOUSE	Solute carrier family 25 (mitochondrial carrier; oxoglutarate carrier), member 11	9	41
Slc25a23	SCMC3_MOUSE	Solute carrier family 25 (mitochondrial carrier; phosphate carrier), member 23	0	7
Slc25a3	MPCP_MOUSE	Solute carrier family 25 (mitochondrial carrier; phosphate carrier), member 3	16	49
Slc25a4	ADT1_MOUSE	Solute carrier family 25 (mitochondrial carrier; adenine nucleotide translocator), member 4	14	60
Slc25a5	ADT2_MOUSE	Solute carrier family 25 (mitochondrial carrier; adenine nucleotide translocator), member 5	13	50
Slc27a1	S27A1_MOUSE	Solute carrier family 27 (fatty acid transporter), member 1	0	10
Slc2a3	GTR3_MOUSE	Solute carrier family 2 (facilitated glucose transporter), member 3	2	11
Slc4a10	S4A10_MOUSE	Solute carrier family 4, sodium bicarbonate transporter, member 10	0	13
Ttyh3	TTYH3_MOUSE	Tweety family member 3	2	13

groups based on literature searches of their presumed functions: 1) G-protein coupled receptors (GPCRs), ion channels, and transporters (Table 3); 2) regulators of protein trafficking, stability, and cytoskeletal anchoring (Table 4); 3) regulators of GTP exchange and protein phosphorylation (Table 5); 4) miscellaneous enzymes (Table 6); and 5) miscellaneous proteins (Table 7). These various binding partners presumably act sequentially to control receptor assembly, forward trafficking in the secretory pathway, trafficking to and stabilization at inhibitory synapses, receptor endocytosis, and endocytic sorting followed by lysosomal or proteosomal degradation.

Cullin1, Ephexin, KCTD12, Mitofusin2, mGluR5, PAK5/7, and Rab5 Bind to the Intracellular Loop of Specific GABA$_A$R Subunits—To confirm our MS findings, we examined the binding of selected hits to the intracellular domains of GABA$_A$R subunits. Our initial studies focused on the GPCR mGluR5 (Grm5), the kinase PAK5/7 (Pak7), the GTPases mitofusin2 (Mfn2), and Rab5, the Rho guanine nucleotide exchange factor ephexin (Ngef) and regulator of ubiquitination cullin1 (Cul1) (Tables 3–5). These proteins were chosen for their range in the total number of peptides identified by MS analysis as follows: from a lower number of peptides (*e.g.* mGluR5; 0 peptides WT

TABLE 4
Regulators of protein trafficking, stability, and cytoskeletal targeting associated with pHα2 identified using GFP-Trap purification

Gene symbol	Reference	Name	Total peptide	
			WT	pHα2
Adam22	ADA22_MOUSE	ADAM metallopeptidase domain 22	0	9
Add3	ADDG_MOUSE	Adducin 3	4	17
Afg3l2	AFG32_MOUSE	AFG3-like AAA ATPase 2	8	42
Cul1	CUL1_MOUSE	Cullin 1	2	22
Cul2	CUL2_MOUSE	Cullin 2	3	17
Cul3	CUL3_MOUSE	Cullin 3	5	21
Dcaf8	DCAF8_MOUSE	DDB1- and CUL4-associated factor 8	0	7
Ddb1	DDB1_MOUSE	Damage-specific DNA-binding protein 1	1	10
Dnaja1	DNJA1_MOUSE	DnaJ heat shock protein family (Hsp40) member A1	2	11
Dync1i2	DC1I2_MOUSE	Dynein, cytoplasmic 1, intermediate chain 2	3	13
Epn1	EPN1_MOUSE	Epsin 1	0	8
Erlin1	ERLN1_MOUSE	Endoplasmic reticulum lipid raft-associated 1	3	13
Exoc3	EXOC3_MOUSE	Exocyst complex component 3	1	18
Exoc7	EXOC7_MOUSE	Exocyst complex component 7	1	28
Exoc8	EXOC8_MOUSE	Exocyst complex component 8	2	13
Hook3	HOOK3_MOUSE	Hook microtubule-tethering protein 3	1	8
Ipo9	IPO9_MOUSE	Importin 9	2	10
Kbtbd7	G5E8C2_MOUSE	Kelch repeat and BTB (POZ) domain containing 7	0	13
Kif3a	KIF3A_MOUSE	Kinesin family member 3A	7	26
Lrrc7	LRRC7_MOUSE	Leucine-rich repeat containing 7	1	7
Magi3	MAGI3_MOUSE	Membrane-associated guanylate kinase, WW, and PDZ domain containing 3	0	14
Mapre2	MARE2_MOUSE	Microtubule-associated protein RP/EB family member 2	0	10
Napa	SNAA_MOUSE	NSF attachment protein α	5	22
Napb	SNAB_MOUSE	NSF attachment protein β	2	15
Nefl	NFL_MOUSE	Neurofilament, light polypeptide	3	11
Ngly1	NGLY1_MOUSE	*N*-Glycanase 1	0	10
Os9	OS9_MOUSE	Osteosarcoma-amplified 9, endoplasmic reticulum lectin	0	8
Psmd9	PSMD9_MOUSE	Proteasome 26S subunit, non-ATPase 9	2	9
Scamp3	SCAM3_MOUSE	Secretory carrier membrane protein 3	0	8
Sec23b	SC23B_MOUSE	Sec23 homolog B, COPII coat complex component	0	9
Sqstm1	SQSTM_MOUSE	Sequestosome 1	1	8
Sv2a	SV2A_MOUSE	Synaptic vesicle glycoprotein 2A	15	64
Sv2b	SV2B_MOUSE	Synaptic vesicle glycoprotein 2B	6	35
Trim32	TRI32_MOUSE	Tripartite motif containing 32	7	24
Uchl1	UCHL1_MOUSE	Ubiquitin C-terminal hydrolase L1	7	22
Usp9x	USP9X_MOUSE	Ubiquitin-specific peptidase 9, X-linked	2	12
Vps35	VPS35_MOUSE	VPS35 retromer complex component	21	69
Vps52	VPS52_MOUSE	VPS52 GARP complex subunit	2	21

TABLE 5
Regulators of GTP exchange and protein phosphorylation associated with pHα2 identified using GFP-Trap purification

Gene symbol	Reference	Name	Total peptide	
			WT	pHα2
Adrbk1	ARBK1_MOUSE	Adrenergic, β, receptor kinase 1	4	27
Arfgef3	BIG3_MOUSE	ARFGEF family member 3	1	11
Atl1	ATLA1_MOUSE	Atlastin GTPase 1	1	8
Dnm1l	DNM1L_MOUSE	Dynamin 1-like	17	61
Elmo1	ELMO1_MOUSE	Engulfment and cell motility 1	0	6
Gnl1	GNL1_MOUSE	Guanine nucleotide-binding protein-like 1	4	15
Gpsm1	GPSM1_MOUSE	G-protein signaling modulator 1	1	14
Iqsec3	IQEC3_MOUSE	IQ motif and Sec7 domain 3	0	13
Lppr4	LPPR4_MOUSE	Phospholipid phosphatase-related 4	8	67
Mfn2	MFN2_MOUSE	Mitofusin 2	8	32
Nedd4l	NED4L_MOUSE	Neural precursor cell expressed, developmentally down-regulated 4-like, E3 ubiquitin protein ligase	1	7
Ngef	NGEF_MOUSE	Neuronal guanine nucleotide exchange factor	5	37
Opa1	OPA1_MOUSE	Optic atrophy 1 (autosomal dominant)	10	32
Pak7	PAK7_MOUSE	p21 protein (Cdc42/Rac)-activated kinase 7	0	6
Ppm1e	PPM1E_MOUSE	Protein phosphatase, Mg^{2+}/Mn^{2+}-dependent 1E	1	7
Ptprd	PTPRD_MOUSE	Protein-tyrosine phosphatase, receptor type D	6	32
Ptprs	PTPRS_MOUSE	Protein-tyrosine phosphatase, receptor type S	6	29
Rab14	RAB14_MOUSE	RAB14, member RAS oncogene family	8	31
Rab1b	RAB1B_MOUSE	RAB1B, member RAS oncogene family	1	8
Rab33b	RB33B_MOUSE	RAB33B, member RAS oncogene family	2	11
Rab5a	RAB5A_MOUSE	RAB5A, member RAS oncogene family	1	11
Rab5b	RAB5B_MOUSE	RAB5B, member RAS oncogene family	0	7
Rhot1	MIRO1_MOUSE	Ras homolog family member T1, Miro1	4	25
Ric8a	RIC8A_MOUSE	RIC8 guanine nucleotide exchange factor A	2	10
Tbc1d15	TBC15_MOUSE	TBC1 domain family member 15	1	8
Tbc1d17	TBC17_MOUSE	TBC1 domain family member 17	2	9

and 6 peptides pHα2) to protein identified by a larger number of peptides (*e.g.* ephexin; 5 peptides WT and 37 peptides pHα2). In addition, GPCRs and the respective activities have all been previously implicated in regulating $GABA_AR$ membrane trafficking (1). Furthermore, we also assessed the interaction of KCTD12 (Table 7), an auxiliary subunit of $GABA_BRs$ previously implicated in regulating $GABA_BR$ signaling and G-protein activation (33). For these experiments, purified GST fusion pro-

TABLE 6
Miscellaneous enzyme activities associated with pHα2 identified using GFP-Trap purification

Gene symbol	Reference	Name	Total peptide	
			WT	pHα2
Acsbg1	ACBG1_MOUSE	Acyl-CoA synthetase bubblegum family member 1	12	39
Acsl3	ACSL3_MOUSE	Acyl-CoA synthetase long-chain family member 3	1	7
Acsl4	ACSL4_MOUSE	Acyl-CoA synthetase long-chain family member 4	2	9
Acss2	ACSA_MOUSE	Acyl-CoA synthetase short-chain family member 2	2	13
Adprh	ADPRH_MOUSE	ADP-ribosylarginine hydrolase	0	6
Aldh18a1	P5CS_MOUSE	Aldehyde dehydrogenase 18 family member A1	6	27
Ca2	CAH2_MOUSE	Carbonic anhydrase II	2	10
Capn2	CAN2_MOUSE	Calpain 2, (m/II) large subunit	2	12
Cds2	CDS2_MOUSE	CDP-diacylglycerol synthase 2	1	15
Cpt1a	CPT1A_MOUSE	Carnitine palmitoyltransferase 1A (liver)	1	13
Dpp3	DPP3_MOUSE	Dipeptidyl-peptidase 3	1	8
Echs1	ECHM_MOUSE	Enoyl-CoA hydratase, short chain, 1, mitochondrial	0	9
Eci1	ECI1_MOUSE	Enoyl-CoA δ isomerase 1	3	11
Gfpt1	GFPT1_MOUSE	Glutamine-fructose-6-phosphate transaminase 1	1	13
Gstz1	MAAI_MOUSE	Glutathione *S*-transferase ζ1	0	6
Gucy1a2	F8VQK3_MOUSE	Guanylate cyclase 1, soluble, α2	4	15
Hsd17b8	DHB8_MOUSE	Hydroxysteroid (17-β) dehydrogenase 8	5	18
Mpst	THTM_MOUSE	Mercaptopyruvate sulfurtransferase	2	9
Mut	MUTA_MOUSE	Methylmalonyl-CoA mutase	3	11
Ndufs1	NDUS1_MOUSE	NADH:ubiquinone oxidoreductase core subunit S1	35	117
Ndufs3	NDUS3_MOUSE	NADH:ubiquinone oxidoreductase core subunit S3	5	19
Pank4	PANK4_MOUSE	Pantothenate kinase 4	1	10
Pfkl	K6PL_MOUSE	Phosphofructokinase, liver	22	68
Plcd1	PLCD1_MOUSE	Phospholipase C δ 1	1	19
Rpn2	RPN2_MOUSE	Ribophorin II	4	13
Srr	SRR_MOUSE	Serine racemase	0	6
Tars	SYTC_MOUSE	Threonyl-tRNA synthetase	9	28

TABLE 7
Miscellaneous proteins associated with pHα2 identified using GFP-Trap purification

Gene symbol	Reference	Name	Total peptide	
			WT	pHα2
Appl1	DP13A_MOUSE	Adaptor protein, phosphotyrosine interaction, PH domain, and leucine zipper containing 1	2	9
Armc10	ARM10_MOUSE	Armadillo repeat containing 10	0	6
Avl9	AVL9_MOUSE	AVL9 homolog (*Saccharomyces cerevisiae*)	4	15
Bcl2l13	B2L13_MOUSE	BCL2-like 13 (apoptosis facilitator)	1	9
Chchd3	CHCH3_MOUSE	Coiled-coil-helix-coiled-coil-helix domain containing 3	2	23
Chchd6	CHCH6_MOUSE	Coiled-coil-helix-coiled-coil-helix domain containing 6	1	13
Clu	CLUS_MOUSE	Clusterin	1	14
Cyc1	CY1_MOUSE	Cytochrome *c*-1	6	25
Eif2b5	EI2BE_MOUSE	Eukaryotic translation initiation factor 2B subunit ϵ	0	19
Fam49a	FA49A_MOUSE	Family with sequence similarity 49 member A	6	23
Fam49b	FA49B_MOUSE	Family with sequence similarity 49 member B	5	22
Fam73b	FA73B_MOUSE	Family with sequence similarity 73 member B	1	7
Hbs1l	HBS1L_MOUSE	HBS1-like translational GTPase	1	9
Immt	IMMT_MOUSE	Inner membrane protein, mitochondrial	40	210
Kctd12	KCD12_MOUSE	Potassium channel tetramerization domain containing 12	0	9
Lhfpl4	LHPL4_MOUSE	Lipoma HMGIC fusion partner-like 4	0	6
Lin7a	LIN7A_MOUSE	Lin-7 homolog A (*Caenorhabditis elegans*)	2	9
Mog	MOG_MOUSE	Myelin oligodendrocyte glycoprotein	1	10
Nbea	NBEA_MOUSE	Neurobeachin	5	37
Pgrmc1	PGRC1_MOUSE	Progesterone receptor membrane component 1	2	10
Phb	PHB_MOUSE	Prohibitin	2	11
Phb2	PHB2_MOUSE	Prohibitin 2	3	11
Plxdc1	PLDX1_MOUSE	Plexin domain containing 1	0	7
Prrt2	PRRT2_MOUSE	Proline-rich transmembrane protein 2	1	7
Samm50	SAM50_MOUSE	SAMM50 sorting and assembly machinery component	1	17
Shisa7	SHSA7_MOUSE	Shisa family member 7	1	8
Tmem132b	F7BAB2_MOUSE	Transmembrane protein 132B	0	6
Ywhab	1433B_MOUSE	Tyrosine 3-monooxygenase/tryptophan 5-monooxygenase activation protein, β	8	28
Ywhag	1433G_MOUSE	Tyrosine 3-monooxygenase/tryptophan 5-monooxygenase activation protein, γ	10	42
Ywhah	1433F_MOUSE	Tyrosine 3-monooxygenase/tryptophan 5-monooxygenase activation protein, η	9	30
Ywhaz	1433Z_MOUSE	Tyrosine 3-monooxygenase/tryptophan 5-monooxygenase activation protein, ζ	11	67
Zer1	ZER1_MOUSE	Zyg-11 related, cell cycle regulator	2	10

teins encoding the intracellular domains of the receptor α1, α2, β3, and γ2 subunits were exposed to detergent-solubilized brain extracts from WT mice, and bound material was subjected to immunoblotting. Cullin1, a component of an E3 ubiquitin ligase complex (34), bound to GST-β3 and γ2 compared with GST alone (Fig. 7*A*; β3 $p < 0.05$, γ2 $p < 0.05$) as did KCTD12 (Fig. 7*C*; β3 $p < 0.05$, γ2 $p < 0.05$). Likewise, mitofusin2, a GTPase localized at the outer mitochondrial membrane (35), bound β3 and γ2 (Fig. 7*D*; β3 $p < 0.001$, γ2 $p < 0.0001$). The GTPase Rab5 is found at endosomes, phagosomes, caveosome, and the plasma membrane (36) and has been shown to colocalize with the GABA$_A$R β3 subunit (37). Consistent with these results, Rab5 bound GST-β3 and γ2 (Fig. 7*G*; β3 $p < 0.0001$, γ2 $p < 0.05$). In contrast to this, PAK5/7, a poorly

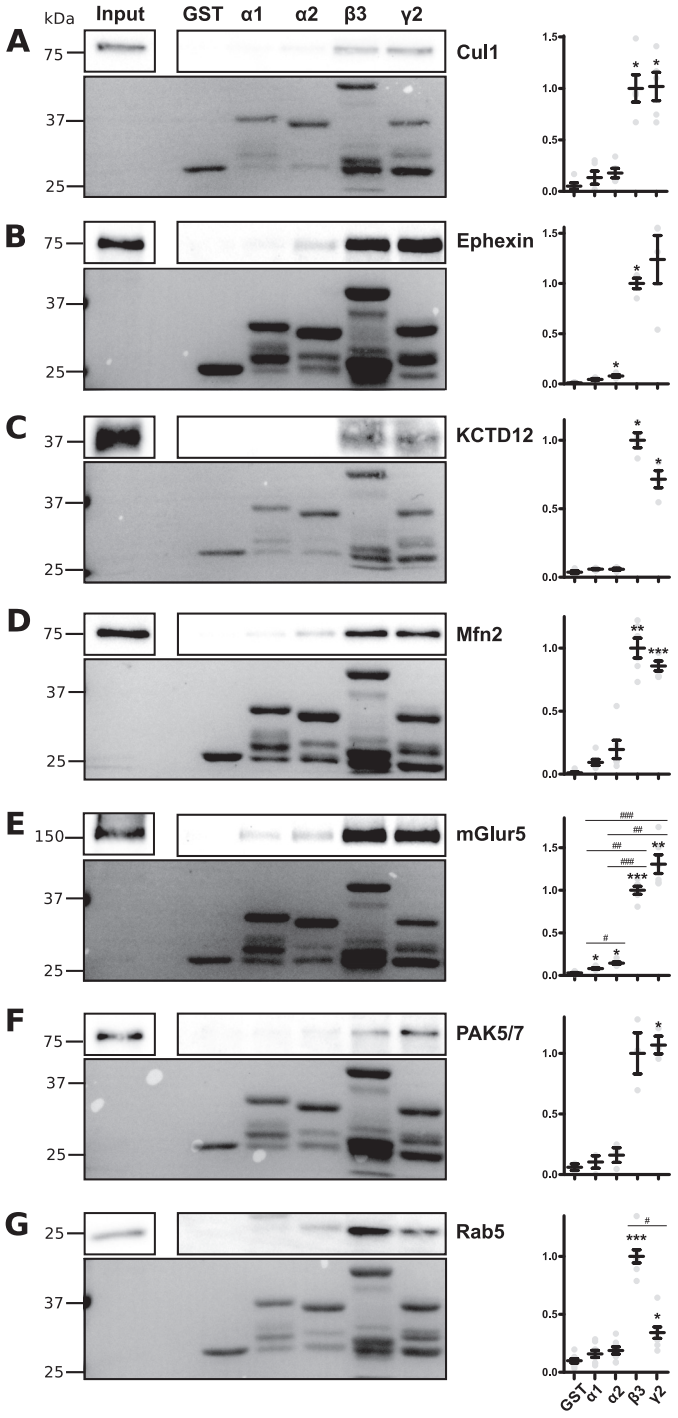

FIGURE 7. **Cullin1, ephexin, KCTD12, mitofusin2, mGluR5, PAK5/7 and Rab5 bind the intracellular loop of specific GABA$_A$Rs.** Detergent-solubilized hippocampal and cortical lysates from WT mice were incubated with GST or GST tagged to the large intracellular loop of various GABA$_A$Rs. Bound proteins including Cul1 (*A*), ephexin (*B*), KCTD12 (*C*), Mfn2 (*D*), mGluR5 (*E*), PAK5/7 (*F*) and Rab5 (*G*) were detected by immunoblotting. The *upper panels* show representative immunoblots; the *lower panels* show Ponceau staining depicting the relative amounts of GST utilized. *Graphs* show pooled quantification of immunoblots. *, $p < 0.05$; **, $p < 0.001$; ***, $p < 0.0001$ compared with GST alone and #, $p < 0.05$; ##, $p < 0.001$; ###, $p < 0.0001$ compared with other subunits, analysis of variance with Games-Howell post hoc test (due to differences in variance), $n = 3–8$. Data are means ± S.E.

described serine/threonine kinase and downstream effector protein for the Rho GTPase Cdc42 (38), bound solely to GST-γ2 (Fig. 7*F*; γ2 $p < 0.05$). Furthermore, the RhoGEF ephexin (39) bound α2 and β3 (Fig. 7*B*; α2 $p < 0.05$, β3 $p < 0.0001$). Finally, the metabotropic glutamate receptor (mGluR5) previously shown to colocalize with GABA$_A$R subunit α1 (40) bound α1, α2, β3, and γ2 (Fig. 7*E*; α1 $p < 0.05$, α2 $p < 0.05$, β3 $p < 0.0001$; γ2 $p < 0.001$). Collectively, these data suggest that proteins that copurify with pHα2 from brain extracts bind to the major intracellular domain of specific GABA$_A$R subunits.

mGluR5, Ephexin, and KCTD12 Coimmunoprecipitate with GABA$_A$Rs—To extend our studies using fusion proteins, detergent-solubilized brains from WT and pHα2 mice were subjected to immunoprecipitation with GFP antibody. Immunoblotting revealed that β3, mGluR5, KCTD12, ephexin, and GFP immunoprecipitated from pHα2 but not WT mice (Fig. 8*A*).

The potential interaction of ephexin with GABA$_A$Rs was of particular interest because ephexin belongs to the same family of GDP-GTP exchange factors (GEFs) as collybistin, a molecule that plays a key role in determining the formation of hippocampal inhibitory synapses (22, 41). To further corroborate our findings in pHα2 mice, we expressed FLAG-ephexin, pHα2, and β3 in HEK293 cells. Reciprocal immunoprecipitation with FLAG and GFP antibodies revealed the robust association of ephexin with GABA$_A$Rs in HEK293 cells (Fig. 8*B*).

Together, these studies demonstrate that proteins identified by mass spectroscopy can be validated in the brain and in expression systems.

Discussion

Inhibitory fast synaptic transmission is critically dependent upon the accumulation and stabilization of selected GABA$_A$R subtypes at inhibitory postsynaptic specializations. To further elucidate the processes neurons utilize to regulate the synaptic accumulation of these critical ligand-gated ion channels, we have created mice in which the α2 subunit is modified with pHluorin and Myc reporters by targeting the respective gene using homologous recombination. These reporters were introduced between residues 4 and 5 of the mature subunit. pHα2 homozygotes were viable and did not exhibit any overt phenotypes but exhibited endogenous fluorescence at inhibitory synapses. Moreover, the properties of sIPSCs and tonic currents, the unitary events that underlie phasic and tonic inhibitory synaptic transmission, were similar between genotypes. Importantly, gephyrin and collybistin, which were previously reported to associate with GABA$_A$R α2 in HEK293 cells (22), could be shown to coimmunoprecipitate in brain lysates, highlighting the necessity for the tagged protein to enable high affinity purifications.

Consensus opinion suggests that the α1–3 subunits are components of synaptic GABA$_A$Rs and that the anxiolytic and sedative properties of benzodiazepines are mediated by specific receptor subtypes containing individual α subunit isoforms. Therefore, we assessed which receptor subunits associate with pHα2 using tandem purification on Myc and GFP antibodies followed by LC-MS/MS. This approach revealed that the pHα2 subunit copurified with α1, α3, α4, α5, β1–3, and γ2 subunits. Using GFP-Trap alone, we further detected association with the γ1, γ3, and δ subunits. Although these results are not quantitative and do not discriminate between surface and intracel-

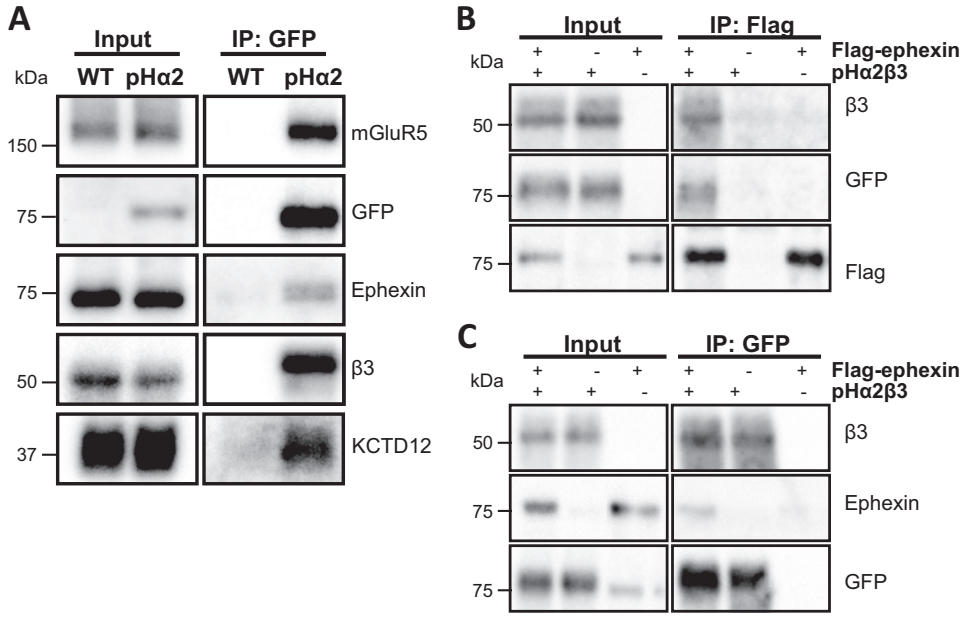

FIGURE 8. **Ephexin, KCTD12, and mGluR5 bind pHα2.** *A,* hippocampal and cortical lysates from WT and pHα2 mice immunoprecipitated with GFP-Trap beads. Bound proteins were immunoblotted with mGluR5, GFP, ephexin, β3, and KCTD12 antibodies. *B* and *C,* transfection of HEK293 cells with a combination of plasmids encoding pHα2, β3, FLAG-ephexin, and empty vector. Cell lysates were immunoprecipitated with FLAG (*B*) or GFP (*C*) and bound proteins were detected by Western blotting.

lular populations, our results do suggest the existence of multiple receptor subtypes with mixed α and/or β subunits, supporting previous observations of the coexistence of different α subunits in a single receptor complex (42–46). Consistent with our results, previous studies to identify proteins associated with the GABA$_A$R α5 subunit through MS analysis exclusively identified other GABA$_A$R subunits, including α1–3, α5, β1–3, and γ2 (47). A more recent investigation into the proteins associated with the GABA$_A$R α1 subunit isolated 18 associated proteins via MS analysis, more than half of which were other GABA$_A$R subunits (48), further supporting the possibility of a more heterogeneous population of receptors than originally predicted (5, 49). It is important to note that some of these subunit interactions may represent "non-productive" or nonfunctional receptor assembly intermediates that are not present on the plasma membrane (1, 2, 25, 50). Because GABA$_A$Rs are a major target for pharmacological agents such as benzodiazepines, barbiturate, neurosteroids, and general anesthetics (3), the heterogeneity of these receptors may have major implications in the design of subunit-selective drugs for therapeutic use.

In addition to receptor subunits, we also isolated the known GABA$_A$R binding partners gephyrin, collybistin, PKC, PKA, and GABA$_B$R2. To the best of our knowledge, this is the first time that these respective protein-protein interactions have been simultaneously demonstrated for GABA$_A$Rs in their native environment. The use of a single GFP-Trap protein purification yielded a 174-multiprotein complex comprising 149 novel protein components that copurified with pHα2 compared with material isolated from WT mice. Novel components of the GABA$_A$R complex include other receptors, proteins required for trafficking, ubiquitination/degradation, GTPases and their regulators, cytoskeletal components, and a host of enzymes. Significantly, the PSD95 family of proteins, which is enriched in excitatory synapses (32), was absent from these purifications.

As an initial means of assessing the significance of our MS experiments, we tested the interaction of selected proteins from brain extracts with GST fusion proteins encoding the intracellular domains of GABA$_A$R subunits. Our studies focused on mGluR5, PAK5/7, mitofusin2, Rab5, ephexin. and cullin1 due to the availability of suitable antibodies. All of the proteins bound to the intracellular domains of the receptor α1, α2, β3, or γ2 subunits, confirming the veracity of our GFP-Trap purifications.

We further validated some of the MS results by demonstrating that mGluR5, KCTD12, and ephexin coIP with pHα2 from brain lysates. We are particularly interested in ephexin due to some similarities with collybistin. Collybistin is a member of the Dbl family of GEFs necessary for the proper clustering of gephyrin and gephyrin-dependent GABA$_A$Rs (41). Like collybistin, ephexin also belongs to the Dbl family of GEFs and therefore has a similar domain structure to collybistin. Studies on ephexin have described its role in axon guidance in retina ganglion cells (13) and dispersal of synaptic acetylcholine receptor clusters in the neuromuscular junction through its capacity to activate Rho family GTPases (51). Numerous regulators of the actin cytoskeleton such as the Rho family GTPases have been demonstrated to be critical for synapse remodeling at excitatory synapses (52). In addition, similar roles for the regulation of the actin cytoskeleton at inhibitory GABAergic synapses have only more recently begun to emerge (53). Although how ephexin, other GTPases, and GTPase regulators identified here may affect GABA$_A$Rs remains to be seen, it is tantalizing to speculate that they may have similarly important roles at inhibitory synapses.

Typical contaminants such as highly abundant proteins (*e.g.* actin, tubulin, and ribosomal proteins) and proteins that bind

unfolded proteins (*e.g.* heat shock proteins) are commonly found in affinity-purified protein preparations (54). Our use of proper WT controls removed many of these contaminants. Furthermore, the requirement for the detection of proteins from three different experiments unveiled protein binding partners that may weakly but stably form a complex with pHα2. Thus, potential pHα2-associated proteins cannot readily be discarded due to a low number of total peptides discovered. Indeed, although only six peptides were identified for mGluR5, we demonstrated that it was robustly coimmunoprecipitated with pHα2 (Fig. 8*A*).

Previously described GABA$_A$R-associated proteins have been demonstrated to be essential for regulatory processes crucial for GABA$_A$R function (1, 2, 55). The characterization of the protein components that form the inhibitory synaptic complex described here have wide-ranging ramifications for the understanding of GABA$_A$R activity and trafficking and therefore its role in synaptic transmission and plasticity. The vast majority of proteins purified here are *novel* putatively GABA$_A$R-associated proteins, indicating that the inhibitory synapse is likely to be far more complex than initially appreciated. Thus, the challenge still remains to elucidate the effects of these associations on GABA$_A$Rs. Considering the crucial role of GABA$_A$R in brain function, it is of fundamental importance to ascertain the underpinning mechanisms that govern these receptors thereby clarifying its role in CNS health and disease.

Author Contributions—Y. N. conducted most of the experiments, analyzed the results, and co-wrote paper. D. H. M. performed PCRs to sequence the mouse and collybistin coIPs, produced GSTs, and provided technical assistance. A. M. performed electrophysiology experiments. D. H. produced GSTs and performed some GST experiments. T. Z. D. performed some electrophysiological experiments. P. A. D. and S. J. M. conceived and coordinated the study and wrote the paper with Y. N. M. J. L. created the pHα2 mouse. All authors analyzed the results and approved the final version of the manuscript.

Acknowledgments—The FLAG-ephexin construct and ephexin antibody were the generous gifts from Prof. Michael Greenberg (Harvard University). The C-terminal anti-α2 antibody was provided by Dr. Verena Tretter and Prof. Werner Sieghart (Medical University of Vienna).

References

1. Jacob, T. C., Moss, S. J., and Jurd, R. (2008) GABA(A) receptor trafficking and its role in the dynamic modulation of neuronal inhibition. *Nat. Rev. Neurosci.* **9,** 331–343
2. Luscher, B., Fuchs, T., and Kilpatrick, C. L. (2011) GABAA receptor trafficking-mediated plasticity of inhibitory synapses. *Neuron* **70,** 385–409
3. Sieghart, W. (2015) Allosteric modulation of GABAA receptors via multiple drug-binding sites. *Adv. Pharmacol.* **72,** 53–96
4. Rudolph, U., and Möhler, H. (2014) GABAA receptor subtypes: therapeutic potential in Down syndrome, affective disorders, schizophrenia, and autism. *Annu. Rev. Pharmacol. Toxicol.* **54,** 483–507
5. Olsen, R. W., and Sieghart, W. (2008) International Union of Pharmacology. LXX. Subtypes of γ-aminobutyric acid(A) receptors: classification on the basis of subunit composition, pharmacology, and function. Update. *Pharmacol. Rev.* **60,** 243–260
6. Patel, B., Mortensen, M., and Smart, T. G. (2014) Stoichiometry of δ subunit containing GABA(A) receptors. *Br. J. Pharmacol.* **171,** 985–994
7. Verdoorn, T. A., Draguhn, A., Ymer, S., Seeburg, P. H., and Sakmann, B. (1990) Functional properties of recombinant rat GABAA receptors depend upon subunit composition. *Neuron* **4,** 919–928
8. Rudolph, U., and Knoflach, F. (2011) Beyond classical benzodiazepines: novel therapeutic potential of GABAA receptor subtypes. *Nat. Rev. Drug Discov.* **10,** 685–697
9. Feng, W., and Zhang, M. (2009) Organization and dynamics of PDZ-domain-related supramodules in the postsynaptic density. *Nat. Rev. Neurosci.* **10,** 87–99
10. Hörtnagl, H., Tasan, R. O., Wieselthaler, A., Kirchmair, E., Sieghart, W., and Sperk, G. (2013) Patterns of mRNA and protein expression for 12 GABAA receptor subunits in the mouse brain. *Neuroscience* **236,** 345–372
11. Brandon, N. J., Jovanovic, J. N., Colledge, M., Kittler, J. T., Brandon, J. M., Scott, J. D., and Moss, S. J. (2003) A-kinase anchoring protein 79/150 facilitates the phosphorylation of GABA(A) receptors by cAMP-dependent protein kinase via selective interaction with receptor β subunits. *Mol. Cell Neurosci.* **22,** 87–97
12. Tretter, V., Jacob, T. C., Mukherjee, J., Fritschy, J. M., Pangalos, M. N., and Moss, S. J. (2008) The clustering of GABA(A) receptor subtypes at inhibitory synapses is facilitated via the direct binding of receptor α2 subunits to gephyrin. *J. Neurosci.* **28,** 1356–1365
13. Shamah, S. M., Lin, M. Z., Goldberg, J. L., Estrach, S., Sahin, M., Hu, L., Bazalakova, M., Neve, R. L., Corfas, G., Debant, A., and Greenberg, M. E. (2001) EphA receptors regulate growth cone dynamics through the novel guanine nucleotide exchange factor ephexin. *Cell* **105,** 233–244
14. Jacob, T. C., Michels, G., Silayeva, L., Haydon, J., Succol, F., and Moss, S. J. (2012) Benzodiazepine treatment induces subtype-specific changes in GABA(A) receptor trafficking and decreases synaptic inhibition. *Proc. Natl. Acad. Sci. U.S.A.* **109,** 18595–18600
15. Abramian, A. M., Comenencia-Ortiz, E., Vithlani, M., Tretter, E. V., Sieghart, W., Davies, P. A., and Moss, S. J. (2010) Protein kinase C phosphorylation regulates membrane insertion of GABAA receptor subtypes that mediate tonic inhibition. *J. Biol. Chem.* **285,** 41795–41805
16. Bolte, S., and Cordelières, F. P. (2006) A guided tour into subcellular colocalization analysis in light microscopy. *J. Microsc.* **224,** 213–232
17. Schneider, C. A., Rasband, W. S., and Eliceiri, K. W. (2012) NIH Image to ImageJ: 25 years of image analysis. *Nat. Methods* **9,** 671–675
18. Candiano, G., Bruschi, M., Musante, L., Santucci, L., Ghiggeri, G. M., Carnemolla, B., Orecchia, P., Zardi, L., and Righetti, P. G. (2004) Blue silver: a very sensitive colloidal Coomassie G-250 staining for proteome analysis. *Electrophoresis* **25,** 1327–1333
19. Mellacheruvu, D., Wright, Z., Couzens, A. L., Lambert, J. P., St-Denis, N. A., Li, T., Miteva, Y. V., Hauri, S., Sardiu, M. E., Low, T. Y., Halim, V. A., Bagshaw, R. D., Hubner, N. C., Al-Hakim, A., Bouchard, A., *et al.* (2013) The CRAPome: a contaminant repository for affinity purification-mass spectrometry data. *Nat. Methods* **10,** 730–736
20. Jacob, T. C., Bogdanov, Y. D., Magnus, C., Saliba, R. S., Kittler, J. T., Haydon, P. G., and Moss, S. J. (2005) Gephyrin regulates the cell surface dynamics of synaptic GABAA receptors. *J. Neurosci.* **25,** 10469–10478
21. Connolly, C. N., Wooltorton, J. R., Smart, T. G., and Moss, S. J. (1996) Subcellular localization of γ-aminobutyric acid type A receptors is determined by receptor β subunits. *Proc. Natl. Acad. Sci. U.S.A.* **93,** 9899–9904
22. Saiepour, L., Fuchs, C., Patrizi, A., Sassoè-Pognetto, M., Harvey, R. J., and Harvey, K. (2010) Complex role of collybistin and gephyrin in GABAA receptor clustering. *J. Biol. Chem.* **285,** 29623–29631
23. Essrich, C., Lorez, M., Benson, J. A., Fritschy, J. M., and Lüscher, B. (1998) Postsynaptic clustering of major GABAA receptor subtypes requires the γ2 subunit and gephyrin. *Nat. Neurosci.* **1,** 563–571
24. Kneussel, M., Brandstätter, J. H., Laube, B., Stahl, S., Müller, U., and Betz, H. (1999) Loss of postsynaptic GABA(A) receptor clustering in gephyrin-deficient mice. *J. Neurosci.* **19,** 9289–9297
25. Connolly, C. N., Krishek, B. J., McDonald, B. J., Smart, T. G., and Moss, S. J. (1996) Assembly and cell surface expression of heteromeric and homomeric γ-aminobutyric acid type A receptors. *J. Biol. Chem.* **271,** 89–96
26. Mukherjee, J., Kretschmannova, K., Gouzer, G., Maric, H. M., Ramsden, S., Tretter, V., Harvey, K., Davies, P. A., Triller, A., Schindelin, H., and

Moss, S. J. (2011) The residence time of GABA(A)Rs at inhibitory synapses is determined by direct binding of the receptor α1 subunit to gephyrin. *J. Neurosci.* **31,** 14677–14687
27. Hoon, M., Soykan, T., Falkenburger, B., Hammer, M., Patrizi, A., Schmidt, K. F., Sassoè-Pognetto, M., Löwel, S., Moser, T., Taschenberger, H., Brose, N., and Varoqueaux, F. (2011) Neuroligin-4 is localized to glycinergic postsynapses and regulates inhibition in the retina. *Proc. Natl. Acad. Sci. U.S.A.* **108,** 3053–3058
28. Poulopoulos, A., Aramuni, G., Meyer, G., Soykan, T., Hoon, M., Papadopoulos, T., Zhang, M., Paarmann, I., Fuchs, C., Harvey, K., Jedlicka, P., Schwarzacher, S. W., Betz, H., Harvey, R. J., Brose, N., *et al.* (2009) Neuroligin 2 drives postsynaptic assembly at perisomatic inhibitory synapses through gephyrin and collybistin. *Neuron* **63,** 628–642
29. Meyer, G., Kirsch, J., Betz, H., and Langosch, D. (1995) Identification of a gephyrin binding motif on the glycine receptor β subunit. *Neuron* **15,** 563–572
30. McDonald, B. J., and Moss, S. J. (1997) Conserved phosphorylation of the intracellular domains of GABA(A) receptor β2 and β3 subunits by cAMP-dependent protein kinase, cGMP-dependent protein kinase protein kinase C and Ca^{2+}/calmodulin type II-dependent protein kinase. *Neuropharmacology* **36,** 1377–1385
31. Balasubramanian, S., Teissére, J. A., Raju, D. V., and Hall, R. A. (2004) Hetero-oligomerization between $GABA_A$ and $GABA_B$ receptors regulates $GABA_B$ receptor trafficking. *J. Biol. Chem.* **279,** 18840–18850
32. Sheng, M., and Kim, E. (2011) The postsynaptic organization of synapses. *Cold Spring Harb. Perspect. Biol.* **3,** a005678
33. Schwenk, J., Metz, M., Zolles, G., Turecek, R., Fritzius, T., Bildl, W., Tarusawa, E., Kulik, A., Unger, A., Ivankova, K., Seddik, R., Tiao, J. Y., Rajalu, M., Trojanova, J., Rohde, V., *et al.* (2010) Native GABA(B) receptors are heteromultimers with a family of auxiliary subunits. *Nature* **465,** 231–235
34. Petroski, M. D., and Deshaies, R. J. (2005) Function and regulation of cullin-RING ubiquitin ligases. *Nat. Rev. Mol. Cell Biol.* **6,** 9–20
35. Stuppia, G., Rizzo, F., Riboldi, G., Del Bo, R., Nizzardo, M., Simone, C., Comi, G. P., Bresolin, N., and Corti, S. (2015) MFN2-related neuropathies: Clinical features, molecular pathogenesis and therapeutic perspectives. *J. Neurol. Sci.* **356,** 7–18
36. Stenmark, H. (2009) Rab GTPases as coordinators of vesicle traffic. *Nat. Rev. Mol. Cell Biol.* **10,** 513–525
37. Smith, K. R., Muir, J., Rao, Y., Browarski, M., Gruenig, M. C., Sheehan, D. F., Haucke, V., and Kittler, J. T. (2012) Stabilization of GABA(A) receptors at endocytic zones is mediated by an AP2 binding motif within the GABA(A) receptor β3 subunit. *J. Neurosci.* **32,** 2485–2498
38. Wells, C. M., and Jones, G. E. (2010) The emerging importance of group II PAKs. *Biochem. J.* **425,** 465–473
39. Shi, L., Fu, A. K., and Ip, N. Y. (2010) Multiple roles of the Rho GEF ephexin1 in synapse remodeling. *Commun. Integr. Biol.* **3,** 622–624
40. Besheer, J., and Hodge, C. W. (2005) Pharmacological and anatomical evidence for an interaction between mGluR5- and GABA(A) α1-containing receptors in the discriminative stimulus effects of ethanol. *Neuropsychopharmacology* **30,** 747–757
41. Papadopoulos, T., Korte, M., Eulenburg, V., Kubota, H., Retiounskaia, M., Harvey, R. J., Harvey, K., O'Sullivan, G. A., Laube, B., Hülsmann, S., Geiger, J. R., and Betz, H. (2007) Impaired GABAergic transmission and altered hippocampal synaptic plasticity in collybistin-deficient mice. *EMBO J.* **26,** 3888–3899
42. del Río, J. C., Araujo, F., Ramos, B., Ruano, D., and Vitorica, J. (2001) Prevalence between different α subunits performing the benzodiazepine binding sites in native heterologous GABA(A) receptors containing the α2 subunit. *J. Neurochem.* **79,** 183–191
43. Benke, D., Fakitsas, P., Roggenmoser, C., Michel, C., Rudolph, U., and Mohler, H. (2004) Analysis of the presence and abundance of GABAA receptors containing two different types of α subunits in murine brain using point-mutated α subunits. *J. Biol. Chem.* **279,** 43654–43660
44. Benke, D., Michel, C., and Mohler, H. (1997) GABA(A) receptors containing the α4-subunit: prevalence, distribution, pharmacology, and subunit architecture *in situ*. *J. Neurochem.* **69,** 806–814
45. Duggan, M. J., Pollard, S., and Stephenson, F. A. (1991) Immunoaffinity purification of GABAA receptor α-subunit iso-oligomers. Demonstration of receptor populations containing α1 α2, α1 α3, and α2 α3 subunit pairs. *J. Biol. Chem.* **266,** 24778–24784
46. Pollard, S., Thompson, C. L., and Stephenson, F. A. (1995) Quantitative characterization of α6 and α1 α6 subunit-containing native γ-aminobutyric acid A receptors of adult rat cerebellum demonstrates two α subunits per receptor oligomer. *J. Biol. Chem.* **270,** 21285–21290
47. Ju, Y. H., Guzzo, A., Chiu, M. W., Taylor, P., Moran, M. F., Gurd, J. W., MacDonald, J. F., and Orser, B. A. (2009) Distinct properties of murine α5 γ-aminobutyric acid type a receptors revealed by biochemical fractionation and mass spectroscopy. *J. Neurosci. Res.* **87,** 1737–1747
48. Heller, E. A., Zhang, W., Selimi, F., Earnheart, J. C., Ślimak, M. A., Santos-Torres, J., Ibañez-Tallon, I., Aoki, C., Chait, B. T., and Heintz, N. (2012) The biochemical anatomy of cortical inhibitory synapses. *PLoS ONE* **7,** e39572
49. Rudolph, U., and Möhler, H. (2004) Analysis of GABAA receptor function and dissection of the pharmacology of benzodiazepines and general anesthetics through mouse genetics. *Annu. Rev. Pharmacol. Toxicol.* **44,** 475–498
50. Gorrie, G. H., Vallis, Y., Stephenson, A., Whitfield, J., Browning, B., Smart, T. G., and Moss, S. J. (1997) Assembly of GABAA receptors composed of α1 and β2 subunits in both cultured neurons and fibroblasts. *J. Neurosci.* **17,** 6587–6596
51. Shi, L., Butt, B., Ip, F. C., Dai, Y., Jiang, L., Yung, W. H., Greenberg, M. E., Fu, A. K., and Ip, N. Y. (2010) Ephexin1 is required for structural maturation and neurotransmission at the neuromuscular junction. *Neuron* **65,** 204–216
52. Tada, T., and Sheng, M. (2006) Molecular mechanisms of dendritic spine morphogenesis. *Curr. Opin. Neurobiol.* **16,** 95–101
53. Smith, K. R., Davenport, E. C., Wei, J., Li, X., Pathania, M., Vaccaro, V., Yan, Z., and Kittler, J. T. (2014) GIT1 and βPIX are essential for GABA(A) receptor synaptic stability and inhibitory neurotransmission. *Cell Rep.* **9,** 298–310
54. Gingras, A. C., Gstaiger, M., Raught, B., and Aebersold, R. (2007) Analysis of protein complexes using mass spectrometry. *Nat. Rev. Mol. Cell Biol.* **8,** 645–654
55. Charych, E. I., Liu, F., Moss, S. J., and Brandon, N. J. (2009) GABA(A) receptors and their associated proteins: implications in the etiology and treatment of schizophrenia and related disorders. *Neuropharmacology* **57,** 481–495